# Femtosecond laser written scattering chip for high-resolution low-cost reconstructive spectrometry

Przemyslaw L. Falak[a], Qi Sun[a], Tom Vettenburg[b], Timothy Lee[a], David B. Phillips[c], Gilberto Brambilla[a], and Martynas Beresna[a]

[a]University of Southampton, Southampton, SO17 1BJ, United Kingdom
[b]University of Dundee, Nethergate, Dundee, DD1 4HN, United Kingdom
[c]University of Exeter, Exeter, EX4 4QL, United Kingdom

## ABSTRACT

The common challenge for reconstructive spectrometers is achieving high spectral resolution without sacrificing device stability, size and costs. Here a fully integrated scattering chip-based spectrometer build on Raspberry Pi platform is designed and implemented. It exhibits no dependence on temperature and humidity (22.7-23.8 °C and 39.5-41 % Rh), is confined in small space (box 50 × 35 × 35 mm) and can reconstruct spectra with resolution up to 0.05 nm (50 pm). The only instability: mechanical micro-movements were compensated by applying pixel binning and device could still reconstruct spectra from binned pictures as small as 32 × 24 pixels.

**Keywords:** Spectrometer, laser-writing, scattering chip, reconstructive spectrometry

## 1. INTRODUCTION

Accurate wavelength and spectrum measurements are a cornerstone principle for various material characterization and analytical methods in many industries, including chemistry, biology, astronomy, materials science, secure printing and forensic analysis. The conventional approach relies on spatially separating wavelengths by angular dispersion and measuring their intensities. However, since spectral separation linearly increases with optical path length between the dispersive element and detector, a high-resolution necessitates sophisticated optical systems or large footprints to lengthen the optical path. Thus to meet the demand for high-resolution yet miniaturized and cheap devices, alternative spectrum measurement techniques are needed.

Here we investigate spectrometers operating using a different paradigm: instead of completely spatially separating each spectral component, each wavelength is mapped to a unique 2D pattern by exploiting the inherent cascaded dispersion from multiple light scattering events. Moreover, high-resolution can be achieved in a tightly confined space because multiple scatterings fold the optical path in the scattering medium.[1] Such setups produce strongly wavelength-dependent 2D speckle-like intensity patterns which appear random but are deterministic, providing the scattering element is stable. Examples of such devices utilizing various scattering media include multimode fiber,[2,3] an integrating sphere,[4] alumina powder[5] and a 2D scattering chip.[6] The reported wavelength measurement resolution was between 13 and 100 pm, but one key challenge persisted: instability.[7] Because high resolution requires the system to be extremely sensitive, even the slightest changes in temperature/humidity, thermal expansion of scattering medium, settling or displacement cause problems with spectral retrieval and requires either frequent re-calibration or operation in controlled environments.[8]

Improved stability can be achieved by embedding scattering medium into a small volume, thus minimizing influence of thermal and environmental gradients. Such a medium, named a scattering chip, can be engineered using femtosecond laser writing[9,10] by focusing fs pulses into a substrate to form nano-voids, which function as scattering spheres, fabricated in close proximity at pre-defined positions without damaging the structure.[11] Here, we demonstrate a high-resolution, low-cost and stable spectrometer based on a laser-written multi-layer scattering chip with nano-voids embedded in silica glass substrate. We investigate its performance and stability both as a wavemeter (single wavelength detection) and spectrometer (spectral measurements).

Further author information: (Send correspondence to P.L.F.)
P.L.F.: E-mail: plf1n15@soton.ac.uk
Q.S.: E-mail: qs3g15@soton.ac.uk

## 2. DESIGN AND FABRICATION

### 2.1 Scattering chip

The scattering chip contains 40 layers of nano-voids spaced 5 µm apart in the $z$ direction (Fig. 1). Using multiple layers increases scattering efficiency by facilitating multiple backwards and forward passes (circa 60% of incident light was scattered).[12] Each individual layer measures 1 × 1 mm with 1000 × 1000 voids (average lateral void separation 1 µm). To increase randomisation of the wavefront, the position of each void in either the horizontal $x$ or vertical $y$ directions was randomized by adding an offset in range ±0.4 µm, alternating direction for each layer. Fabrication time was 5 min per layer. High purity fused silica (UVFS C7980 0F) with low thermal expansion and OH content of 800-1000 ppm (high environmental stability)[13] was used as the substrate.

Voids were formed by focusing into the substrate $\lambda = 515$ nm wavelength pulses generated as the second harmonic from a $\lambda = 1.03$ µm femtosecond laser system (Pharos, Light Conversion Ltd., Lithuania) with 200 kHz repetition rate and 200 fs pulse duration. A 1.25 NA oil-immersion focusing objective was used on a $z$ stage, with the substrate (10 × 10 × 1 mm) on an $x$-$y$ stage for translation perpendicular to the writing beam direction. An overhead CMOS camera allowed visual inspection in-situ of the written structure.

### 2.2 Enclosure assembly

Spectrometer consisting of the scattering chip, imaging module and collimator were attached to 3D printed enclosure. The importance of the spectrometer enclosure cannot be underestimated, as it must: (1) accommodate key device components in a compact space to minimise device footprint, (2) maximise stability by shielding interior from fluctuating environmental conditions (including temperature, humidity and ambient light) and (3) provide mechanical protection for delicate electronic parts.

The box was 3D printed from Tough PLA (Ultimaker) with dimensions of 57 × 35 × 35 mm (Fig. 1b), and includes mounting space and protection for all components, a retainer fixing the camera to prevent its displacement during measurements, an adjustable holder for the scattering chip and a removable top cover for access. Because fluctuating temperature and humidity may affect scattering process via swelling or thermal expansion,[14,15] a temperature/humidity sensor was included to facilitate environmental stability analysis.

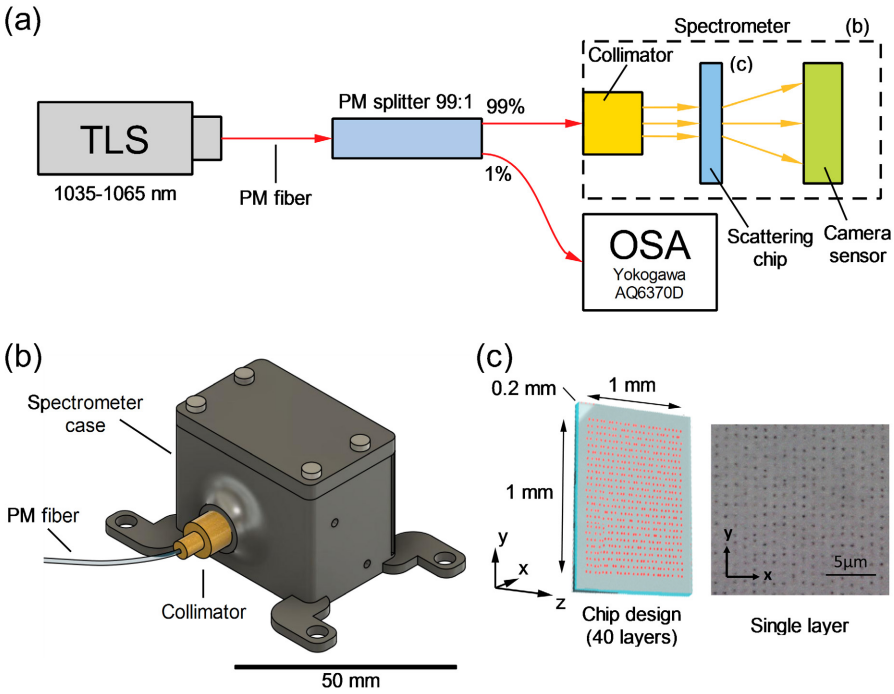


Figure 1. (a) Experimental set-up for spectrometer calibration and characterization, (b) Spectrometer body, (c) Scattering chip design.

## 3. METHOD OF OPERATION

### 3.1 Experimental set up

The reconstructive spectrometer operates on the spatial-to-spectral mapping principle.[16,17] Initial calibration is performed by recording speckle patterns for different wavelengths. Next, during measurement, the system captures the speckle pattern of an unknown wavelength or spectrum and finds the correlation factors between the measured and previously obtained calibration reference patterns. The highest correlation factors indicate which reference patterns correspond most with the measured ones, and hence the measured wavelength(s) can be identified.[18,19]

The experimental set-up for both calibration and measurement demonstration are the same (Fig. 1a): a tunable laser source (TLS) with wavelength range 1035-1065 nm, ∼40 pm linewidth, 1 mW output power and optical signal-to-noise ratio of 40 dB was used, with the smallest tuning step ($\Delta\lambda$) of 0.05 nm. The TLS was connected by polarisation-maintaining (PM) single mode fiber to a 99:1 PM splitter coupler (which also filtered through polarisation in the slow axis). The output from the 99% port was fed via PM fiber to the collimator inside the spectrometer case (Sec. 2.2). The collimated beam passed through the scattering chip, with the resulting speckle pattern acquired by a CMOS camera with near-infrared sensitivity (Raspberry Pi NoIR Camera V2). The 1% splitter output port was delivered via single mode fiber to a commercial optical spectral analyser (OSA) Yokogawa AQ6370D to determine the calibration wavelength. As the TLS was tuned to each wavelength in the range, a speckle pattern $I(x, y)$ was captured via the camera as a 640 × 480 pixel array (single pixel size of 1.12 × 1.12 μm). Such resolution was selected as a good balance between speckle visibility and computational speed.

### 3.2 Spectral reconstruction technique

To reconstruct spectrum, each speckle was reshaped into column vector $M$ which has 307,200 pixel elements (total number of a 640 × 480 pixel speckle pattern). By comparing the tested (measured) data $T(M, r)$ against the calibrated (reference) dataset $C(M, \lambda)$ the spectral information can be revealed.[20,21] The calibration data contains vectorized speckle patterns obtained during calibration for individual wavelengths ($\lambda$). The tested data structure is similar, yet it contains only $r$ speckle patterns collected during wavelengths measurement. By using Eq. (1) the degree of correlation $S$ can be evaluated between each test and calibration speckle patterns. Therefore, by finding the highest correlation coefficient, the most likely wavelength for the measured data can be identified and its value implies the relative intensity of wavelength. Therefore, such system can work as either wavemeter (single wavelength) or spectrometer (multiple wavelengths at time).

$$T(M, r) = C(M, \lambda) * S \tag{1}$$

Since the Eq. (1) represents in fact linear set of equations it can be written more succinctly as matrix equation: $T = CS$. Assuming noise-free measurement,[22] the spectral correlations matrix $S$ can be obtained from the following relation: $S = C^{-1}T$. The $C^{-1}$ is the Moore-Penrose pseudo-inverse of matrix $C$, which can be calculated from the singular value decomposition: $C = U\Sigma V^T$ as $C^{-1} = V\Sigma^{-1}U^T$.[23–25] $U$ and $V$ are unitary matrices, $\Sigma$ is a diagonal matrix with the singular values and $^T$ denotes the matrix transpose. Each singular value represents an independent link between the wavelengths and their effect on the measured speckle pattern.

## 4. RESULTS AND DISCUSSION

### 4.1 Stability analysis

Instability is a key problem preventing high-resolution scattering spectrometers from wider applications. Ideally, speckle pattern intensity distributions should be a function of source wavelength only. However, varying environmental conditions can alter the speckle pattern intensity distribution or cause translational displacement, which can invalidate the original calibration patterns[26] and reduces spectral reconstruction accuracy and repeatability. To quantify the stability, three metrics were analysed over time for fixed input spectrum/wavelength: (i) reconstructed wavelength over time, (ii) root mean square (RMS) difference between speckle patterns, and (iii) transformation matrix between speckle patterns.

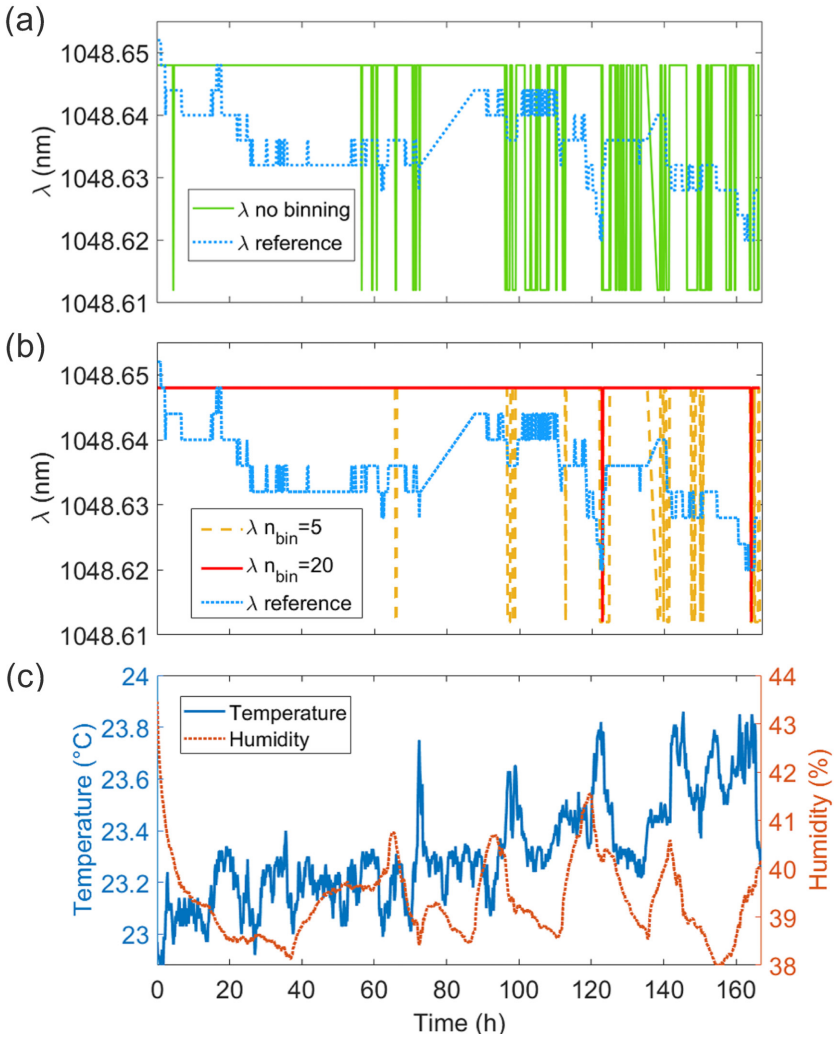


Figure 2. Single-wavelength temporal stability of the device and impact of applying binning: (a) 1-week reconstruction of single wavelength with no binning applied and reference wavelength measured by OSA Yokogawa 6370D, (b) single-wavelength reconstruction with $n_{\text{bin}} = 5$ and $n_{\text{bin}} = 20$ binning applied, (c) Environmental stability: temperature and humidity vs. time. The tuning step of the laser source used during calibration process was 50 pm.

The first method directly checks stability of a reconstructed wavelength over time, as shown in 2a. After initial calibration, a single fixed wavelength is used as the input. The spectrometer periodically captures speckle patterns from which it reconstructs the wavelength, which is compared against the reference wavelength measured by the commercial optical spectrum analyser (OSA) in parallel. Whilst the reconstructed wavelength is relatively stable, there are 0.05 nm fluctuation "detunings" due to the fact that this was the minimum calibration source tuning step $\Delta\lambda$, and so the reconstruction algorithm matches the tested speckle pattern either to the "correct" reference wavelength or to its neighbour. While the temperature and humidity varied as shown in Fig. 2c during the test (22.7-23.8 °C and 38-43 % humidity), there appeared to be no significant effect on the reconstructed wavelength.

To quantify the variation between the speckle patterns, the RMS difference was calculated between the initial (reference) and each subsequently captured speckle patterns (each pattern is first normalized, i.e. divided by its maximum value). The bigger the RMS, the more different the speckle patterns, whereas if system is perfectly stable, RMS equals zero. For 72 h measurements, the RMS difference oscillated in range 0.022-0.025, implying relatively stable and similar speckle patterns.

Whilst the RMS allows overall quantification of stability, it cannot distinguish whether this is due to an unstable scattering chip or physical displacements of the camera. However, by finding the transformation matrix needed to best match the initial reference speckle pattern with each subsequently captured test pattern, such movements can be tracked. This utilizes intensity-based registration[27] to reveal any translation in the $x$ and $y$ (horizontal and vertical) directions as well as any rotation.[28] This would verify the camera displacement contribution to any RMS variation and as a result determine stability of scattering chip. 72 h measurements confirmed no rotation (the angle was smaller than 0.06° due to the registration error and limitation of approximating the transformation matrix) and displacements were purely translational. Whilst speckle patterns were relatively stable in the horizontal direction (oscillating by $\pm 0.25$ pixel), the vertical movements fluctuated rapidly within the range of $\pm 1.25$ pixel and were identified as the main source of instability due to micro-mechanical movements caused by thermal swelling/expanding of the camera box material.

### 4.2 Binning for improved stability

The stability analysis (Sec. 4.1) revealed the key source of instability: translational speckle pattern displacement. To mitigate its impact, pixel binning of the speckle pattern images was investigated, in which groups of $n_{\text{bin}} \times n_{\text{bin}}$ pixels, where $n_{\text{bin}} > 1$ is the binning order, were combined into super-pixels by summing their intensity values. The resulting pictures retain the shape of characteristic pattern of the original speckle but with reduced pixel resolution (Fig. 3(a)). This method improves the reconstruction algorithm's tolerance to displacement since new pixels were created by summing up ("collapsing") the neighboring pixels values. Furthermore, as increased binning reduces image size, it improves data-processing speed and reduces memory requirements. As a result, the only major concern is remaining within the threshold where binned pictures still retain enough characteristic pattern information to faithfully reconstruct the spectrum/wavelength.

The single wavelength reconstruction stability test (Fig. 2(a)) revealed fluctuations in the measurement. By applying binning (Fig. 2(b)) of $n_{\text{bin}}$=5 (speckle pattern image reduced to 128 × 96 pixels) and $n_{\text{bin}}$=20 (32 × 24 pixels), the number of fluctuations is reduced - from 87 (no binning) up to only 2 for $n_{\text{bin}}$=20, which indicates high stability over the 1-week temporal measurement.

To further quantify the impact of binning, the spectrum correlation matrices $S$ (Eq.(1)) were visualised for single wavelength measurements in range 1035-1065 nm with tuning step 0.05 nm (Fig. 3(b)). Increasing binning order results in unchanged background, but the main diagonal of matrices is becoming less intense and finally blurs with the background (maximum binning threshold). Furthermore, the standard error between reconstructed and reference wavelengths has been calculated for binning orders from 1 (no binning) to 20 (Fig. 3(c)). Initially, the error is high (0.16 nm) but when binning increases, it goes down to a minimum value near 0.05 nm (this is the lowest limit, equal to the source tuning step $\Delta\lambda$) for $n_{\text{bin}} = 5$ and oscillates near this value until binning is excessive, which again causes error to rise (reaching maximum binning threshold).

### 4.3 Spectral reconstruction stability

Whilst wavemeter resolution is defined as the distance between neighbouring sampling points, equal to the $\Delta\lambda$ calibration source tuning step, the spectral resolution of the system is the minimum separation between neighbouring wavelengths which can be distinguished and therefore is equal to doubled wavemeter resolution (100 pm) since at least three sampling points must exist to separate two neighbouring wavelengths (Fig. 4(a)).

Binning can be applied for spectral measurements as well, which reduces amount of data to process for reconstruction but there is a limit: whilst low-order binning maintains the shape of the reconstructed spectrum (Fig. 4(b)) and standard spectral intensity error equals only 4.9 % ($n_{\text{bin}}$=5), a higher binning order can cause reconstructed spectral peaks and troughs to become flatter due to reduced correlation for each wavelength intensity, and hence reconstruction error increases (reaching 14 % at $n_{\text{bin}}$=20). In this case, $n_{\text{bin}}$=5 or lower would offer a reasonable trade-off between improved stability and acceptably small intensity error.

## 5. CONCLUSION

Multiple scattering reconstructive spectrometers are extremely sensitive to incoming wavelengths and hence can detect the slightest change in light frequency. However, their instability limits the potential application and

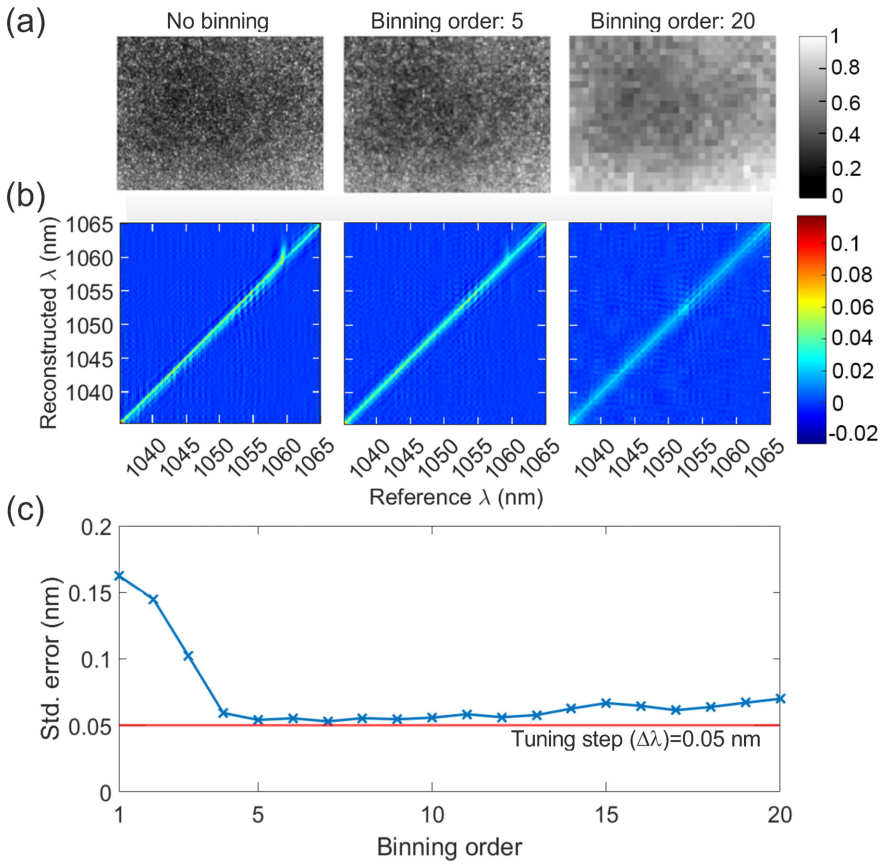


Figure 3. Binning effect on: (a) speckle patterns intensity profiles, (b) Spectrum matrices $S$, (c) Spectrum reconstruction standard error vs. binning order $n_{\text{bin}}$ from 1 (no binning) to 20. Red line indicates 0.05 nm - the tuning step of the laser source.

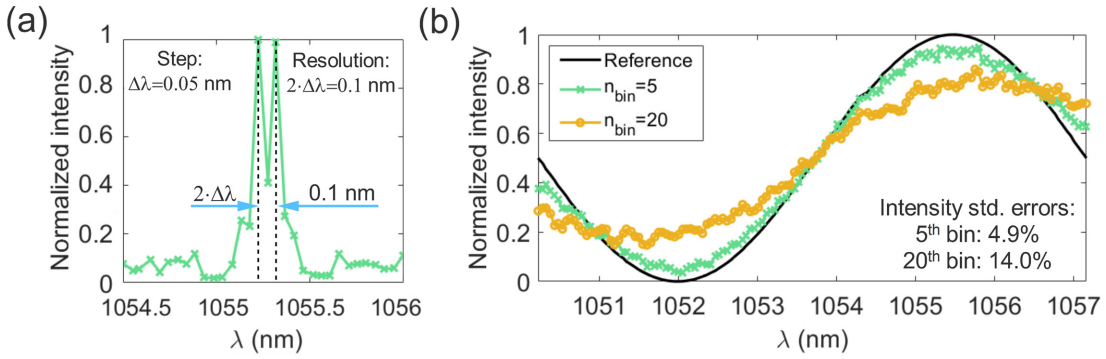


Figure 4. (a) Spectral resolution of device: 0.1 nm as the smallest separation distance between two neighbouring wavelengths, (b) Effect of excessive binning on the spectrum shape.

long-term performance. Therefore, we demonstrated a much more stable, compact, and low cost device, based on a tailored scattering medium written by a fs-laser. The designed 1 × 1 mm scattering chip with 40-layers confines scattering voids in a small volume, making the system more stable than previously reported devices, and the 1-week test showed single wavelength reconstruction varied only by 50 pm (tuning step). Indeed, the stability analysis revealed that fluctuating environmental conditions (22.7-23.8 °C and 38-43 % humidity) had minimal systematic impact on the spectrometer. The device resolution is limited by the tuning step of light source used during calibration ($\Delta\lambda$=50 pm). That is why the spectrometer resolution equals 100 pm and it can be further improved if finer tuning steps of the calibration source are used. To analyze the speckle pattern stability for single wavelength input for 3 days we calculated displacement and RMS difference between speckle patterns. Such quantification revealed vertical translational movements over 1.5 pixels range which were main source of the instability caused by micro-mechanical movements. In order to reduce their impact, picture binning was applied. By repeating single wavelength measurements with speckle patterns binned into 32 × 24 pixels, the reconstructed wavelength remained stable all the time during measurement (from 87 to 2 fluctuations). Whilst binning is a suitable technique to improve stability for single wavelength measurement (wavemeter), it should be used with caution during spectral measurements (spectrometer). For low binning order, we observe low standard error in the reconstructed spectral intensity (4.9% for $n_{\mathrm{bin}} = 5$), but excessive binning causes spectrum flattening and standard error increases (14.0% for $n_{\mathrm{bin}} = 20$).

## ACKNOWLEDGMENTS

M.B., D.B.P., T.V. and G.B. directed the project, Q.S. and P.L.F. carried out the wavemeter, spectrometer and stability experiments, P.L.F. designed the spectrometer case, T.V., T.L., Q.S. and P.L.F. developed the analysis algorithm. P.L.F. wrote the manuscript. This work is supported by by the EPSRC Advanced Metrology Hub, Huddersfield with the pilot-study grant "Compact Tailored Spectrometer". T.V. is a UKRI Future Leaders Fellow supported by grant MR/S034900/1.

## REFERENCES

[1] Redding, B., Liew, S. F., Sarma, R., and Cao, H., "On-chip random spectrometer," in [*Applied Industrial Optics: Spectroscopy, Imaging and Metrology*], AM2A–4, Optical Society of America (2014).

[2] Redding, B., Popoff, S. M., and Cao, H., "All-fiber spectrometer based on speckle pattern reconstruction," *Opt. Express* **21**(5), 6584–6600 (2013).

[3] Emadi, A., Wu, H., de Graaf, G., and Wolffenbuttel, R., "Design and implementation of a sub-nm resolution microspectrometer based on a linear-variable optical filter," *Opt. Express* **20**(1), 489–507 (2012).

[4] Metzger, N. K., Spesyvtsev, R., Bruce, G. D., Miller, B., Maker, G. T., Malcolm, G., Mazilu, M., and Dholakia, K., "Harnessing speckle for a sub-femtometre resolved broadband wavemeter and laser stabilization," *Nat. Commun.* **8**(1), 1–8 (2017).

[5] Mazilu, M., Vettenburg, T., Di Falco, A., and Dholakia, K., "Random super-prism wavelength meter," *Opt. Lett.* **39**(1), 96–99 (2014).

[6] Redding, B., Liew, S. F., Sarma, R., and Cao, H., "Compact spectrometer based on a disordered photonic chip," *Nat. Photonics* **7**(9), 746–751 (2013).

[7] Bruce, G. D., O'Donnell, L., Chen, M., and Dholakia, K., "Overcoming the speckle correlation limit to achieve a fiber wavemeter with attometer resolution," *Opt. Lett.* **44**(6), 1367–1370 (2019).

[8] Liu, T. and Fiore, A., "Designing open channels in random scattering media for on-chip spectrometers," *Optica* **7**(8), 934–939 (2020).

[9] Glezer, E., Milosavljevic, M., Huang, L., Finlay, R., Her, T.-H., Callan, J. P., and Mazur, E., "Three-dimensional optical storage inside transparent materials," *Opt. Lett.* **21**(24), 2023–2025 (1996).

[10] Zhang, J., Čerkauskaitė, A., Drevinskas, R., Patel, A., Beresna, M., and Kazansky, P. G., "Eternal 5D data storage by ultrafast laser writing in glass," in [*Laser-based Micro- and Nanoprocessing X*], Klotzbach, U., Washio, K., and Arnold, C. B., eds., **9736**, 163 – 178, International Society for Optics and Photonics, SPIE (2016).

[11] Glezer, E. N. and Mazur, E., "Ultrafast-laser driven micro-explosions in transparent materials," *Appl. Phys. Lett.* **71**(7), 882–884 (1997).

[12] Sun, Q., Vettenburg, T., Lee, T., Phillips, D., Beresna, M., and Brambilla, G., "Compact spectrometer chips based on fs laser written multi-layer scattering medium," in [*Asia Commun. Photonics Conf. ACP 2019*], *Asia Commun. Photonics Conf. ACP 2019* , T4D.5, Optical Society of America (2019).

[13] Drotning, W. D., "Thermal expansion of glasses in the solid and liquid phases," *Int. J. Thermophys.* **6**(6), 705–714 (1985).

[14] Casalini, T., Rossi, F., Castrovinci, A., and Perale, G., "A perspective on polylactic acid-based polymers use for nanoparticles synthesis and applications," *Front. Bioeng. Biotechnol.* **7**, 259 (2019).

[15] Faust, J. L., Kelly, P. G., Jones, B. D., and Roy-Mayhew, J. D., "Effects of coefficient of thermal expansion and moisture absorption on the dimensional accuracy of carbon-reinforced 3d printed parts," *Polymers* **13**(21) (2021).

[16] Yang, Z., Albrow-Owen, T., Cai, W., and Hasan, T., "Miniaturization of optical spectrometers," *Science* **371**(6528), eabe0722 (2021).

[17] Goshtasby, A. A., [*Image registration: Principles, tools and methods*], Springer Science & Business Media (2012).

[18] Xu, Z., Wang, Z., Sullivan, M. E., Brady, D. J., Foulger, S. H., and Adibi, A., "Multimodal multiplex spectroscopy using photonic crystals," *Opt. Express* **11**(18), 2126–2133 (2003).

[19] Redding, B., Popoff, S. M., Bromberg, Y., Choma, M. A., and Cao, H., "Noise analysis of spectrometers based on speckle pattern reconstruction," *Appl. Opt.* **53**(3), 410–417 (2014).

[20] Shih, F., "Mathematical preliminaries," in [*Image Processing and Pattern Recognition*], 17–39, John Wiley & Sons, Ltd (2010).

[21] Chan, T. and Shen, J., "Some modern image analysis tools," in [*Image Processing and Analysis*], 31–89, Society for Industrial and Applied Mathematics (2005).

[22] Chan, T. and Shen, J., "Image denoising," in [*Image Processing and Analysis*], 145–206, Society for Industrial and Applied Mathematics (2005).

[23] Baksalary, O. M. and Trenkler, G., "The moore–penrose inverse: a hundred years on a frontline of physics research," *Eur. Phys. J. H* **46**(1), 9 (2021).

[24] Sadek, R. A., "Svd based image processing applications: State of the art, contributions and research challenges," *Int. J. Adv. Comput. Sci. Appl.* **3**(7) (2012).

[25] Brunton, S. and Kutz, J., "Singular value decomposition (svd)," in [*Data-driven Science and Engineering: Machine Learning, Dynamical Systems, and Control*], 3–46, Cambridge University Press (2019).

[26] Goshtasby, A. A., [*2-D and 3-D image registration: for medical, remote sensing, and industrial applications*], John Wiley & Sons (2005).

[27] Styner, M., Brechbuhler, C., Szckely, G., and Gerig, G., "Parametric estimate of intensity inhomogeneities applied to mri," *IEEE Trans. Med. Imag.* **19**(3), 153–165 (2000).

[28] Guizar-Sicairos, M., Thurman, S. T., and Fienup, J. R., "Efficient subpixel image registration algorithms," *Opt. Lett.* **33**(2), 156–158 (2008).